Int. J. Heat Mass Transfer. Vol. 24, No. 10, pp. 1711–1722, 1981
Printed in Great Britain

0017-9310/81/101711-12 $02.00/0

AN IMPROVED QUASI-STEADY APPROACH FOR TRANSIENT CONJUGATED FORCED CONVECTION PROBLEMS

JAMES SUCEC
Professor of Mechanical Engineering, Rm. 203 Boardman Hall,
University of Maine, Orono, ME 04473, U.S.A.

(*Received* 16 *September* 1980 *and in revised form* 16 *April* 1981)

Abstract—A method is presented, namely the improved quasi-steady approach, which takes into approximate account both the effect of thermal history and of thermal energy storage capacity of a flowing fluid in transient, conjugated, forced convection problems and thus dispenses with two of the assumptions ordinarily implicit in the usual, simple quasi-steady approach to such problems. The development of the improved approach is suggested by a transformation of variable which leads to an exact solution for slug flows which is then generalized and asserted to be approximately valid for non-slug flows.

Two analytical solutions using the proposed approach are presented and compared to finite difference solutions which were generated as benchmarks for the comparison. Additional comparisons are made to the usual, standard quasi-steady results.

NOMENCLATURE

a, $=\rho c_p R/\rho_w c_{pw} b$, ratio of thermal storage capacity of the fluid to that of the solid;
Ai, Airy function defined as shown in equation (33);
A_s, defined by equation (41);
b, thickness of duct wall;
b^*, $=\rho_w c_{pw} bR\omega/k$;
B_c, defined by equation (42);
c, constant, $=\frac{9}{2}(0.538)\Gamma\left(\frac{2}{3}\right)\left(\frac{2}{3}\right)^{2/3}$;
c_0, constant, $=0.538\,\Gamma\left(\frac{2}{3}\right)$;
c_p, c_{pw}, specific heat of fluid and duct wall respectively;
G, G_s, defined by equations (20) and (19), respectively;
k, thermal conductivity of the fluid;
K, modified Bessel function of the second kind;
n, integer;
q_w, local surface heat flux;
Q_w, $=-q_w R\chi^{1/3}/3\ (0.538)\ \Gamma\ (2/3)k\Delta T$, non-dimensional local surface heat flux with $\Delta T = \theta_e$ for a step change of inlet temperature and $\Delta T = \Delta T_0$ for a sinusoidal inlet temperature;
R, half thickness of duct;
s, Laplace transform parameter;
t, time;
T, T_i, local and initial temperatures, respectively;
u, u_m, u_{max}, local, mass average, and maximum velocity in duct, respectively;
x, y, space coordinates along duct and normal to wall, respectively;
Z, defined by equation (16).

Greek symbols

α, $=k/\rho c_p$ thermal diffusivity of fluid;
Γ, Gamma function;
Δt, time increment;
ΔT_0, amplitude of sinusoidal inlet temperature variation;
$\Delta x, \Delta y$, space increments along duct and perpendicular to wall, respectively;
θ, $=T - T_i$, temperature excess over initial temperature;
θ_{w0}, refers to a constant wall temperature excess;
ρ, ρ_w, mass density of fluid and of wall, respectively;
σ, defined by equation (13);
χ, $=\alpha x/R^2 u_m$ non-dimensional distance along duct;
τ, defined by equation (3);
ω, angular frequency;
ϕ_0, $=0.538(3)^{1/3}\Gamma(2/3)k/\rho_w c_{pw} bR$.

Subscripts and superscripts

B, local bulk mean temperature of fluid;
e, refers to inlet conditions;
i, j, indices locating position of node in x and y, respectively;
k, index specifying time;
sqs, standard quasi-steady approach;
w, refers to conditions in the solid duct wall material.

INTRODUCTION

A KNOWLEDGE of the time varying surface temperature and heat flux for a solid, over which or through which a fluid flows, is important during the starting up and shutting down phases, or when a change in operating level occurs between different steady-state levels. In

addition, this knowledge is also needed for devices which may never attain steady-state operation because it is in their nature to operate periodically in time. Examples of physical equipment which experience these types of unsteady operating conditions include regenerative and recuperative heat exchangers, the blades and vanes of gas turbine power plants, and nuclear reactor fuel rods.

In the most realistic analyses of solid surfaces interacting by convection with a fluid during a transient, cognizance is given to the fact that the conditions at the solid–fluid interface are not known *a priori*, but rather what is known as a function of time is a boundary condition at some other surface of the solid, or generation within the solid, or perhaps an inlet fluid temperature. Problems of this type in which the temperature field in the moving fluid and the temperature field in the bounding solid must be found simultaneously, because of the mutual coupling of the fields, are referred to as conjugate problems. Generally speaking, the complexity of a transient conjugated problem is such that often an approximate solution using the standard, simple quasi-steady approach is decided upon. Basically, this quasi-steady approach utilizes a steady-state surface coefficient of heat transfer which is a constant in both space and time or which exhibits the functional dependency on space coordinates which is valid for an isothermal surface. Thus, the standard quasi-steady approach does not account for the thermal history effect, that is, the surface temperature's dependence upon position, or for the effect of thermal energy storage capacity of the flowing fluid. Representative of this type of approach to a transient conjugated problem is the analytical portion of the work in [1] by Adams and Gebhart.

Because of the relative analytical simplicity it affords, the slug flow idealization has been employed in the solution to a number of transient conjugate problems. In [2], Siegel and Perlmutter consider laminar slug flow in a channel with arbitrarily specified surface heat flux. Exact solutions are found and these are used by [3] in an energy balance on the wall to yield an exact solution to a slug flow conjugate problem where the transient is caused by various types of generation inside the wall material. Namatame [4] presents a modified quasi-steady solution for a slug flow transient conjugated problem in which the thermal history effect is taken into account. Sucec, as part of [5], uses a surface heat flux expression for arbitrary surface temperature in a modified quasi-steady solution of a slug flow conjugated problem in which the fluid inlet temperature varies with time.

Soliman and Johnson [6, 7], find approximate solutions for the case of turbulent flow over a plate with thermal capacity when the plate generation is a step function or an exponential in time. First they find a solution for the instantaneous surface coefficient of heat transfer for the zero capacity plate when the convective terms in the thermal energy equations are neglected. Then the assumption is made that this time varying surface coefficient also applies to the finite capacity plate for $t < x/u_m$ and that the steady-state surface coefficient is the proper one for $t > x/u_m$. With this, the energy balance on the plate is solved for the time varying average surface temperature. Comparisons with experimental data indicated much better agreement than yielded by the standard, simple quasi-steady results. In an approach bearing some similarity to the work of [6] and [7], Kawamura [8, 9], employs an approximate expression for the eddy diffusivity of heat which allows an analytical solution of the transient thermal energy equation with convective terms absent when the fluid interacts with a wall, of non-zero thermal capacity, which undergoes a step change in generation. The time varying surface coefficient of heat transfer thus found is then used in the thermal energy equation with the convective term present, until the surface coefficient drops to the steady state value after which the steady-state surface coefficient of heat transfer is used. Both these approaches, [6–9], represent attempts to take into account the thermal capacity of the fluid, something the standard quasi-steady approach does not do.

Both Dorfman [10], and Karvinen [11, 12], describe a modified quasi-steady approach, for flow over a flat plate, in which thermal history is taken into approximate account by use of surface heat flux expressions that are valid for steady-state conditions when the surface temperature distribution is an arbitrary function of the space coordinate. Energy balances on the wall which incorporate these surface heat flux expressions can then be solved for the unknown wall temperature distribution.

The present work concerns itself with the development and application of an improved quasi-steady approach for transient conjugated forced convection problems which takes into approximate account both thermal history and the thermal capacity of the flowing fluid. This improved quasi-steady method has its origins in the slug flow problem and is, in fact, an exact solution to the slug flow problem which, after extension and generalization, yields approximate expressions for the surface heat flux in non-slug flows which account for thermal history and fluid thermal capacity. The method is applied to two problems of flow in a parallel plate duct in which the finite thermal capacity walls and fluid are both at a constant temperature initially when a transient is initiated by either a step change in fluid inlet temperature with time, or a sinusoidal variation in time. For a linear velocity profile, exact solutions are found for the improved quasi-steady approach by application of Laplace transformations. Presented, for these two different inlet temperature variations, are the response functions for the wall temperature, wall heat flux and local bulk mean temperature of the fluid flowing in the duct. In order to test the validity of the improved quasi-steady approach, finite difference solutions were generated to serve as baseline solutions or benchmarks. The comparison of the finite difference results

with those of the improved quasi-steady analysis also serves to delineate the domain of applicability, with acceptable accuracy, of the improved quasi-steady approach. Finally, also for comparison purposes, some results for the standard quasi-steady method are presented.

ANALYSIS

Development of the improved quasi-steady approach

Since, as mentioned earlier, the method proposed herein evolved from a solution to a slug flow problem, we begin by considering a fairly general slug flow problem, namely the steady, laminar, slug flow of a fluid in a parallel plate duct of height $2R$ with the fluid initially at a constant temperature when suddenly the temperature of the duct walls becomes an arbitrary function of position and time and the fluid inlet temperature begins varying arbitrarily with time. The problem, at this point, is to develop an expression for the local, instantaneous, surface heat flux. The mathematical description of the slug flow problem becomes as follows:

$$\frac{\partial\theta}{\partial t} + u_m\frac{\partial\theta}{\partial x} = \alpha\frac{\partial^2\theta}{\partial y^2}, \tag{1}$$

$$t = 0,\ x > 0,\ 0 \le y \le R \quad \theta = 0,$$

$$x = 0,\ t > 0,\ 0 \le y \le R \quad \theta = \theta_e(t),$$

$$t > 0,\ x > 0,\ y = R \quad \frac{\partial\theta}{\partial y} = 0 \tag{2}$$

$$\text{and at } y = 0 \quad \theta = \theta_w(x, t).$$

One improvement to the standard, simple quasi-steady approach would be to solve the above set of equations with $\partial\theta/\partial t$ set equal to zero, yet retaining $\theta_w(x, t)$ at $y = 0$. The resultant expression for the surface heat flux now takes into account thermal history and is given by Sucec [5] for flow over a flat plate. In effect, this is also what Karvinen [11], and Dorfman [10] do for the case of non-slug flow over a plate. However, in an effort to retain the dependence of flux on the fluid's thermal capacity, it was decided to use the following transformation due to Schumann [13]:

$$\tau = t - x/u_m. \tag{3}$$

Using this in a formal change of variables and leaving open the question of satisfaction of the initial condition on time, equations (1) and (2) become, with $\theta = \theta(x, y, \tau)$,

$$u_m\frac{\partial\theta}{\partial x} = \alpha\frac{\partial^2\theta}{\partial y^2}, \tag{4}$$

$$\text{all } \tau\begin{cases} x = 0, & 0 \le y \le R \quad \theta = \theta_e(\tau) \\ x > 0; & y = R, \quad \dfrac{\partial\theta}{\partial y} = 0 \text{ and at} \\ & y = 0, \quad \theta = \theta_w(x, \tau + x/u_m). \end{cases} \tag{5}$$

The Laplace transformation with respect to x is employed to solve equations (4) and (5) which map into (6) and (7) with $\bar{\theta}$ defined as follows.

$$\bar{\theta} = \underset{x\to s}{L}\ \theta(x, y, \tau) = \int_0^\infty \theta e^{-sx}\,dx,$$

$$\frac{d^2\bar{\theta}}{dy^2} - \frac{su_m}{\alpha}\bar{\theta} = -\frac{u_m}{\alpha}\theta_e(\tau), \tag{6}$$

$$y = R \quad \frac{d\bar{\theta}}{dy} = 0, \quad \text{and at } y = 0, \quad \bar{\theta} = \bar{\theta}_w(s, \tau). \tag{7}$$

Upon solution of (6) subject to the conditions (7), one arrives at,

$$\bar{\theta} = \left[\frac{\theta_e(\tau)}{s} - \theta_w(s, \tau)\right]\left[\tanh\left(R\sqrt{\frac{u_m s}{\alpha}}\right)\right.$$

$$\left.\times \sinh\left(y\sqrt{\frac{u_m s}{\alpha}}\right) - \cosh\left(y\sqrt{\frac{u_m s}{\alpha}}\right)\right] + \frac{\theta_e(\tau)}{s}. \tag{8}$$

The transformed surface heat flux q_w can be found from (8) as

$$\bar{q}_w = -k\left(\frac{d\bar{\theta}}{dy}\right)_{y=0} = k\sqrt{\frac{u_m}{\alpha}}\,\frac{\tanh\left(R\sqrt{\frac{u_m s}{\alpha}}\right)}{\sqrt{s}}$$

$$\times\left[s\bar{\theta}_w(s, \tau) - \theta_e(\tau)\right]. \tag{9}$$

The inverse Laplace transform of the first factor in (9) is given in [14] and when this is used in the convolution integral with the inverse of the factor in brackets, the following results:

$$q_w(x, \tau) = \frac{k}{R}\int_0^x \frac{\sum_{n=-\infty}^{\infty}(-1)^n e^{-[u_m R^2 n^2/\alpha(x-\xi)]}}{\sqrt{\frac{\pi\alpha(x-\xi)}{u_m R^2}}}$$

$$\times\frac{\partial\theta_w}{\partial\xi}\left(\xi, \tau + \frac{\xi}{u_m}\right)d\xi. \tag{10}$$

Now since $\theta_w(x, t)$ one notes from (10) that $\tau + \xi/u_m$, by its placement in the argument of $\partial\theta_w/\partial\xi$, is acting like a dummy variable for time t. Since physically, we are considering only time $t > 0$, it follows that:

$$\tau + \frac{\xi}{u_m} \ge 0, \tag{11}$$

or that, using (3) in (11)

$$\xi \ge x - u_m t. \tag{12}$$

Since ξ, a dummy variable for x, must lie between 0 and x, it follows that equation (12) gives rise to two different time domains. If $t > x/u_m$ then (12) is automatically satisfied for all ξ between 0 and x, whereas if $t < x/u_m$ then ξ must begin at $x - u_m t$ to ensure that it will always be positive.

Thus for $t < x/u_m$, the lower limit of the integral in equation (10) must be $x - u_m t$. It is convenient to use the following change in variable in equation (10), when $t < x/u_m$, to cause q_w to be viewed as a function of τ and t:

$$\sigma = t - x/u_m + \xi/u_m. \tag{13}$$

With this, the solution for the surface heat flux in the original slug flow problem, equations (1) and (2), becomes as follows where the integrals are to be intrepeted as Stieltjes integrals:

$$q_w(\tau, t) = \frac{k}{R}\int_0^t \left[\frac{\sum_{n=-r}^{r}(-1)^n e^{-[R^2n^2/\alpha(t-\sigma)]}}{\sqrt{\frac{\pi\alpha(t-\sigma)}{R^2}}}\right] \times \frac{\partial\theta_w}{\partial\sigma}(\tau,\sigma)\,d\sigma, \quad \text{for } t \le x/u_m, \tag{14}$$

$$q_w(x, \tau) = \frac{k}{R}\int_0^x \left[\frac{\sum_{n=-r}^{r}(-1)^n e^{-[R^2u_mn^2/\alpha(x-\xi)]}}{\sqrt{\frac{\pi\alpha(x-\xi)}{u_mR^2}}}\right] \times \frac{\partial\theta_w}{\partial\xi}(\xi,\tau)\,d\xi, \quad \text{for } t \ge x/u_m. \tag{15}$$

The two different time domains that appear in equations (14) and (15) are the same ones as deduced for slug flows by Siegel and Perlmutter [2] on the basis of a Lagrangian viewpoint and physical reasoning. Depending upon whether $t < x/u_m$ or $t > x/u_m$ one is dealing with fluid downstream or upstream, respectively, of the front of fluid that was at $x = 0$ at $t = 0$.

The condition at $t = 0$ in equation (2), which was not satisfied explicitly by the solution to (4) and (5), is satisfied implicitly by equation (14) because of the arguments which led to (14). This can be established rigorously by using the following transformation:

$$Z = x - u_m t. \tag{16}$$

Viewing $\theta = \theta(Z, y, t)$, equations (1) and (2) transform to the following:

$$\frac{\partial\theta}{\partial t} = \alpha\frac{\partial^2\theta}{\partial y^2}, \tag{17}$$

$$\text{all } Z\begin{cases} t = 0; & 0 \le y \le R; \quad \theta = 0; \\ t > 0; & y = R\dfrac{\partial\theta}{\partial y} = 0 \text{ and at} \\ & y = 0, \quad \theta = \theta_w(Z, t). \end{cases} \tag{18}$$

If one solves equation (17) subject to conditions (18) which include the initial condition at $t = 0$, one is led quite directly to equation (14). Equations (14) and (15) are the surface heat flux manifestations of the complete exact solution and these two equations can now be used directly in an energy balance on a wall which bounds the fluid. The energy balance equation, when solved, gives the exact solution for the unknown wall temperature in a transient conjugated slug flow duct problem.

Extension to non-slug flows

Now the most difficult transient conjugated problems, which are also the ones of most interest from the practical viewpoint, are the ones involving a non-slug velocity profile and for fully developed, hydrodynamically, duct flow this means that $u = u(y)$. In order to extend and generalize equations (14) and (15) to non-slug flows, equation (10) is examined. Consider steady-state conditions and an isothermal wall. Integrating equation (10) under these conditions where the integration must be done in the Stieltjes sense one arrives at,

$$q_w(x) = G_s(x)\theta_{w0} \text{ (steady and isothermal conditions)}, \tag{19}$$

where $G_s(x)$ is the kernel of equation (10). Thus, the kernels of equations (14) and (15), $G_s[u_m(t-\sigma)]$ and $G_s(x-\xi)$, have their form dictated by the solution for the steady-state flux on an isothermal surface, equation (19).

Next, it is asserted that equations (14) and (15) will hold approximately in non-slug flows if the kernels in the integrands come from the appropriate non-slug flow solution. Thus, if a solution or an experimental correlation is available, as many already are in Kays textbook [15], for the surface heat flux in steady, non-slug flow over an isothermal surface in the form

$$q_w(x) = G(x)\theta_{w0}, \tag{20}$$

then equations (14) and (15) are written as follows:

$$q_w(\tau, t) = \int_0^t G[u_m(t-\sigma)]\frac{\partial\theta_w}{\partial\sigma}(\tau,\sigma)\,d\sigma, \quad \text{for } t < x/u_m, \tag{21}$$

$$q_w(x, \tau) = \int_0^x G(x-\xi)\frac{\partial\theta_w}{\partial\xi}(\xi,\tau)\,d\xi, \quad \text{for } t > x/u_m. \tag{22}$$

Equations (21) and (22) constitute the surface heat flux expressions to be used in the improved quasi-steady approach being advanced here. These expressions take into approximate account both thermal history and finite thermal capacity of the fluid and reduce to the exact expressions for slug flow when the G function is replaced by the G_s for slug flow from equation (19). The generalized expressions (21) and (22) form a structure that unifies and displays the complementary aspects of previous work on modified quasi-steady approaches since the researchers in [6] and [8] focused on the effect of fluid thermal energy capacity, while those of [4], [5], [10], and [11] concentrated on the effect of thermal history alone.

The approximate nature of the equations (21) and (22) for non-slug flows is partially rooted in the fact that there are not only two time domains, as in slug flows, but one would probably define three time domains. The first time domain $t < x/u_{max}$ is very similar to that in a slug flow since it consists of fluid that was already in the channel when the transient was initiated, that is, fluid which satisfies the initial condition. At some time greater than x/u_{max}, essentially all of the fluid that satisfied the initial condition has

already been transported past the x of interest and hence one is considering fluid that satisfies the inlet boundary condition and the state is reasonably similar to that of the second time domain $t > x/u_m$ of a slug flow. However, in the non-slug flow with $u = u(y)$ there is a third or intermediate time domain in which the slower moving fluid near the wall, which satisfies the initial condition, is communicating by thermal conduction with the faster moving fluid above it at the same x, fluid that satisfies the inlet boundary condition. The duration of this intermediate time regime compared with the length of the first and second time domains will have an effect on the accuracy of the improved quasi-steady method in non-slug flow problems. One can obtain some qualitative information about this complication by looking at the thermal energy equation, for a fully developed non-slug velocity profile, using as independent variables x, y, and τ, which has the form

$$\left[1 - \frac{u(y)}{u_m}\right]\frac{\partial\theta}{\partial\tau} + u(y)\frac{\partial\theta}{\partial x} = \alpha\frac{\partial^2\theta}{\partial y^2}. \tag{23}$$

The improved quasi-steady analysis assumes that the first term on the left side of equation (23) is essentially zero. Obviously, in the case of slug flow where $u(y) = u_m$ this is rigorously true. Even in a non-slug flow case this may be essentially true if $\partial\theta/\partial\tau$, or $[1 - u(y)/u_m]$, or their product, is small. The factor $[1 - u(y)/u_m]$ will be small for relatively 'square' non-slug velocity profiles and is seen to take on its largest values near the wall which, of course, is the region where it takes longest to sweep away the fluid which satisfies the initial condition. Some evidence for the adequacy of a two time domain approach when the non-slug velocity profile is 'square' enough is implicit in [6], where an external turbulent flow was considered, and also in [16] where laminar flow inside ducts is considered. Thus, it was decided to use as the approximate signal time, or lag time, which separates the two time domains in the improved quasi-steady model, the same quantity that is appropriate for a slug flow, namely x/u_m.

Application of the improved quasi-steady model

To test the validity of, and learn more about, the proposed approximate model, it was applied to two problems. Considered was steady, laminar, constant property, fully developed hydrodynamically, flow in a parallel plate duct of height $2R$ with walls, of thickness b, which are perfectly insulated on their outside surfaces when both the walls and the fluid are originally at a constant temperature. In the first case considered, a transient was initiated in the flowing fluid and the walls by a step change in the fluid inlet temperature while in the second case the unsteadiness is caused by a fluid inlet temperature that varies sinusoidally with time for all $t > 0$. The problem is to predict the surface temperature and heat flux as well as the bulk mean temperature of the fluid as functions of x and t.

An energy balance is made on a control volume of the duct wall b by dx, assuming that the wall temperature can be lumped in the y direction, that axial conduction in the wall is negligibly small, and that the thermal properties of the wall are constant, and yields the following.

$$\frac{\partial\theta_w}{\partial t} + \frac{q_w}{\rho_w c_{pw} b} = 0. \tag{24}$$

The improved quasi-steady expressions for the surface heat flux, q_w, are given by equations (21) and (22) where the function $G(x)$ must now be chosen. At this point, for a combination of reasons, a linear in y velocity profile was chosen. Firstly, it provides analytical convenience in allowing an exact solution with the $G(x)$ function given implicitly in the results of Lighthill [17]. (The correct, but more complicated, $G(x)$ for the actual quadratic velocity profile is available in [15]). Secondly, the linear velocity profile is thought to provide the most severe test of the improved quasi-steady procedure since it is farther away from the slug profile than is the more 'square' actual quadratic velocity profile in the duct and one of the primary reasons for these solutions is to test the accuracy of the model. Also, as is well known, the linear velocity profile is an adequate representation of the actual velocity profile in a thin thermal boundary layer. Thus, with the use of the wall shear stress and mass average velocity u_m appropriate to the actual quadratic, fully developed laminar duct flow, the linear velocity profile becomes

$$u(y) = 3u_m\frac{y}{R}. \tag{25}$$

Lighthill's result for the steady state flux in [17] is an exact solution for a linear velocity profile and is applicable here, certainly in the thermal entrance region. Hence, in terms of the non-dimensional distance $\chi = \alpha x/u_m R^2$, we have that,

$$G(\chi) = 0.538(3)^{1/3}\frac{k}{R}\frac{1}{\chi^{1/3}}. \tag{26}$$

With $\theta_w = T_w - T_i$ and therefore $\theta_w = 0$ at $t = 0$, it is seen by inserting equation (21) into (24) that the solution in the first time domain, $t < x/u_m$, is $\theta = 0$. Insertion of (26) into (22) and this result used in (24) gives the equation to be solved for the surface temperature distribution in the second time domain as, after noting that $\partial\theta_w/\partial t = \partial\theta_w/\partial\tau$,

$$\frac{\partial\theta_w}{\partial\tau} + \frac{0.538(3)^{1/3}k}{\rho_w c_{pw} bR}\int_0^\chi \frac{1}{(\chi - \xi)^{1/3}} \times \frac{\partial\theta_w}{\partial\xi}[\xi, \tau]\,d\xi = 0 \quad \text{for } \tau \geqq 0. \tag{27}$$

Solution for step change in inlet temperature

The solution to equation (27) for θ_w must satisfy the following two side conditions,

$$\tau = 0, \quad \chi > 0, \quad \theta_w = 0, \quad \text{and } \chi = 0, \quad \tau > 0, \quad \theta_w = \theta_e. \quad (28)$$

Taking the Laplace transform of equation (27) with respect to χ yields,

$$\frac{d\bar{\theta}_w}{d\tau} + \frac{\phi_0}{s^{2/3}}(s\bar{\theta}_w - \theta_e) = 0, \quad (29)$$

$$\tau = 0, \quad \bar{\theta}_w = 0. \quad (30)$$

Solution of (29) subject to (30) yields the transformed function as

$$\frac{\bar{\theta}_w}{\theta_e} = \frac{1}{s} - \frac{1}{s} e^{-\phi_0 s^{1/3}\tau}. \quad (31)$$

The procedure for finding the inverse transform of (31) is given in Appendix A and yields the following.

$$\frac{\theta_w(\chi,\tau)}{\theta_e} = 1 - \frac{1}{6\pi\chi^{3/2}} \int_{\phi_0\tau}^{\infty} \times u^{3/2}(u - \phi_0\tau)^2 K_{1/3}\left(\frac{2}{3}\frac{u^{3/2}}{\sqrt{3\chi}}\right) du. \quad (32)$$

One check that can be made on the operations that led to (32) consists of seeing if (32) does yield $\theta_w = 0$ at $\tau = 0$. Setting $\tau = 0$ in (32) leads to an infinite integral available in analytical form in Luke [18] and its value causes the initial condition to be satisfied. However, for values of τ other than zero, it was found that equation (32) was more easily worked with when it was recast in a form in which the Airy function, $Ai(z)$ appeared. From [19], one has that

$$Ai(z) = \frac{1}{\pi}\sqrt{\frac{z}{3}} K_{1/3}\left(\frac{2}{3}z^{3/2}\right). \quad (33)$$

Using this yields the following solution for the wall temperature distribution by the improved quasi-steady approach.

$$\frac{\theta_w}{\theta_e} = 0 \quad \text{for } t < x/u_m$$

$$\frac{\theta_w}{\theta_e} = 1 - \frac{3}{2}\int_{\phi_0\tau/(3\chi)^{1/3}}^{\infty} z\left[z - \frac{\phi_0\tau}{(3\chi)^{1/3}}\right]^2 \times Ai(z)\,dz, \quad \text{for } \tau \geq 0. \quad (34)$$

Now the non-dimensional surface heat flux can be found from (24) after changing the variable to τ and rearranging to give

$$Q_w(\chi,\tau) = \int_{\phi_0\tau/(3\chi)^{1/3}}^{\infty} z\left[z - \frac{\phi_0\tau}{(3\chi)^{1/3}}\right]^2 \times Ai(z)\,dz, \quad \text{for } \tau \geq 0, \quad (35)$$

with Q_w being zero for $t < x/u_m$.

In order to arrive at the bulk mean temperature excess θ_B of the fluid, one makes an energy balance on a control volume dx long by R high which gives

$$q_w = \rho u_m c_p R\frac{\partial\theta_B}{\partial x} + \rho c_p R\frac{\partial\theta_B}{\partial t}. \quad (36)$$

Changing the variables to χ and τ in (36) and then solving for θ_B yields

$$\frac{\theta_B(\chi,\tau)}{\theta_e} = 1 + \frac{R}{k\theta_e}\int_0^{\chi} q_w(\beta,\tau)\,d\beta. \quad (37)$$

If one obtains q_w from (35) and inserts it into (37), the result contains an inner integral whose lower limit depends upon the integration variable of the outer integral. However, if one then integrates by parts three times the resulting equation contains only integrals of the same general form as already present in (34) and gives θ_B as follows:

$$\frac{\theta_B(\chi,\tau)}{\theta_e} = 1 - c\chi^{2/3}\int_{\phi_0\tau/(3\chi)^{1/3}}^{\infty} Ai(z) \times \left\{z^2 + \left[\frac{\phi_0\tau}{(3\chi)^{1/3}}\right]^2 - 2z\frac{\phi_0\tau}{(3\chi)^{1/3}}\right\} dz, \quad \text{for } \tau \geq 0, \quad (38)$$

and

$$\theta_B = 0 \quad \text{for } t < x/u_m.$$

Sinusoidal inlet temperature variation

Considered next is a problem similar to the one in the previous section except that now the transient is initiated by a fluid temperature that varies sinusoidally at the inlet. In this case there is never a steady-state since, after the transient portion of the unsteadiness decays, one is left with the ultimate periodic unsteady-state.

Once again the fluid and the duct walls are at constant initial temperature excess $\theta_i = 0$ when the inlet fluid temperature excess, at $t = 0$, begins varying with time as $\theta_e = \Delta T_0 \sin \omega t$.

Application of the improved quasi-steady approach to this problem leads to equation (27) which, after application of the Laplace transform, gives the temperature excess in the transformed plane as

$$\frac{\bar{\theta}_w}{\Delta T_0} = \frac{\sin\omega\tau}{s^{1/3}\left(s^{2/3} + \frac{\omega^2}{\phi_0^2}\right)} - \frac{\cos\omega\tau}{s^{2/3}\left(\frac{\phi_0}{\omega}s^{2/3} + \frac{\omega}{\phi_0}\right)} + \frac{e^{-\phi_0 s^{1/3}\tau}}{s^{2/3}\left(\frac{\phi_0}{\omega}s^{2/3} + \frac{\omega}{\phi_0}\right)}. \quad (39)$$

To effect the inversion back to the physical plane the same overall procedure was used as given earlier for equation (31). Thus, one gets:

$$\frac{\theta_w(b^*\chi^{1/3}, \omega\tau)}{\Delta T_0} = \left[\frac{\sqrt{(3)}\Gamma(1)\Gamma(2/3)3^{2/3}c_0^2}{2\pi(b^*\chi^{1/3})^2} - 3\left(\frac{c_0}{b^*\chi^{1/3}}\right)^2 \times \int_0^{\infty} z\,Ai(z)\cos\left(\frac{b^*\chi^{1/3}z}{c_0}\right)dz\right] \times \sin\omega\tau - \left[\frac{3^{3/2}\Gamma(1)\Gamma(4/3)3^{1/3}c_0}{2\pi b^*\chi^{1/3}}\right.$$

$$- 3\left(\frac{c_0}{b^*\chi^{1/3}}\right)^2 \int_0^{\infty} z\,Ai(z) \times \sin\left(\frac{b^*\chi^{1/3}z}{c_0}\right)\mathrm{d}z\Bigg]\cos\omega\tau + \frac{3c_0}{b^*\chi^{1/3}} \times \int_{c_0\omega\tau/b^*\chi^{1/3}}^{\infty}\left\{z - \frac{c_0\omega\tau}{b^*\chi^{1/3}} - \frac{c_0}{b^*\chi^{1/3}} \times \sin\left[\frac{b^*\chi^{1/3}}{c_0}\left(z - \frac{c_0\omega\tau}{b^*\chi^{1/3}}\right)\right]\right\} \times z\,Ai(z)\,\mathrm{d}z, \quad \text{for } \tau \geqq 0, \text{ and}$$

$$\theta_w/\Delta T_0 = 0 \text{ for } t < x/u_m. \tag{40}$$

The first two terms of (40) represent the eventual periodic unsteady response while the last term is the transient portion of the response. After defining $A_s(\chi)$ and $B_c(\chi)$, equations (40), (24), and (37), with ΔT_0 replacing θ_e, give the flux and bulk mean temperature as follows:

$$A_s(\chi) = \text{coefficient of } \sin\omega\tau \text{ in equation (40)}, \tag{41}$$

$$B_c(\chi) = \text{coefficient of } \cos\omega\tau \text{ in equation (40)}, \tag{42}$$

$$Q_w(b^*\chi^{1/3}, \omega\tau) = \frac{b^*\chi^{1/3}B_c(\chi)}{3c_0}\sin\omega\tau + \frac{b^*\chi^{1/3}A_s(\chi)}{3c_0} \times \cos\omega\tau + \frac{c_0}{b^*\chi^{1/3}}\int_{c_0\omega\tau/b^*\chi^{1/3}}^{\infty} \times \left\{-1 + \cos\left[\frac{b^*\chi^{1/3}}{c_0}\left(z - \frac{c_0\omega\tau}{b^*\chi^{1/3}}\right)\right]\right\} \times z\,Ai(z)\,\mathrm{d}z, \quad \text{for } \tau \geqq 0, \text{ and}$$

$$Q_w = 0 \quad \text{for } t < x/u_m, \tag{43}$$

$$\frac{\theta_B(b^*\chi^{1/3}, \omega\tau) - \sin\omega\tau}{\Delta T_0} = \frac{6c_0^3}{b^{*2}}\Bigg[\int_0^{\infty} Ai(z) \times \sin\left(\frac{b^*\chi^{1/3}z}{c_0}\right)\mathrm{d}z - \frac{\sqrt{(3)}\Gamma(2/3)b^*\chi^{1/3}}{2\pi c_0 3^{1/3}}\Bigg] \times \cos\omega\tau + \frac{6c_0^3}{b^{*2}}\left\{\int_0^{\infty} Ai(z)\left[1 - \cos\left(\frac{b^*\chi^{1/3}z}{c_0}\right)\right]\mathrm{d}z - \frac{3^{3/2}\Gamma(1)\Gamma(4/3)b^{*2}\chi^{2/3}}{4\pi c_0^2 3^{2/3}}\right\}\sin\omega\tau - \frac{3(2/3)^{2/3}c_0^2}{b^*}\int_0^{\chi}\beta^{-2/3}\int_{c_0\omega\tau/b^*\beta^{1/3}}^{\infty} \times \left\{-1 + \cos\left[\frac{b^*\beta^{1/3}}{c_0}\left(z - \frac{c_0\omega\tau}{b^*\beta^{1/3}}\right)\right]\right\} \times z\,Ai(z)\,\mathrm{d}z\,\mathrm{d}\beta, \quad \text{for } \tau \geqq 0, \text{ and}$$

$$\theta_B = 0 \quad \text{for } t < x/u_m. \tag{44}$$

Standard quasi-steady approach

For comparison purposes, the same problems will also be solved by the commonly employed standard quasi-steady model which normally uses the heat transfer coefficient for steady state flow over an isothermal surface. This is given by equation (26) for the cases considered here. Using this in (24) gives the wall temperature and flux as follows for step and sinusoidal inlet temperature variations, respectively:

$$\frac{\theta_{w_{sqs}}}{\theta_e} = 1 - \mathrm{e}^{-1.0651\{[\phi_0\tau/(3\chi)^{1/3}] + 0.72851\,\alpha\chi^{2/3}\}}, \tag{45}$$

$$Q_{w_{sqs}}(\chi, \tau) = \frac{1.0651}{3}\left[1 - \frac{\theta_{w_{sqs}}}{\theta_e}\right], \tag{46}$$

$$\frac{\theta_{w_{sqs}}}{\Delta T_0} = \Bigg\{\sin(\omega\tau + \omega x/u_m) + 1.2888\,b^*\chi^{1/3} \times \Bigg[-\cos(\omega\tau + \omega x/u_m) + \frac{\mathrm{e}^{-0.7759\{(\omega\tau/b^*\chi^{1/3}) + [(\omega x/u_m)/b^*\chi^{1/3}]\}}}{1 + 1.6609\,b^{*2}\chi^{2/3}}\Bigg]\Bigg\}, \tag{47}$$

$$Q_{w_{sqs}} = 0.45756\,b^*\chi^{1/3}\Bigg\{\cos(\omega\tau + \omega x/u_m) + 1.2888\,b^*\chi^{1/3}\sin(\omega\tau + \omega x/u_m) - \frac{\mathrm{e}^{-0.7759\{(\omega\tau/b^*\chi^{1/3}) + [(\omega x/u_m)/b^*\chi^{1/3}]\}}}{1 + 1.6609\,b^{*2}\chi^{2/3}}\Bigg\}. \tag{48}$$

Finite difference equations

To ascertain the accuracy and the limitations of the improved quasi-steady approach, it was decided to compare it to the true solution of the problem as represented by a finite difference solution to the governing partial differential equations (23) and (24) with the velocity profile given by (25). Energy balances on nodal volumes, equivalent to use of the standard central difference approximation for the conduction term and an 'upwind' scheme for the convective term, gave the implicit finite difference algorithms below:

$$\begin{aligned}
&\text{for } j = 1: && (\Delta R + 1)\phi_{i,1}^{k+1} - \Delta R\phi_{i,2}^{k+1} = \phi_{i,1}^{k} \\
&2 \leq j \leq N-1: && -\Delta F\phi_{i,j-1}^{k+1} + (2\Delta F + \Delta c + 1)\phi_{i,j}^{k+1} - \Delta F\phi_{i,j+1}^{k+1} = \phi_{i,j}^{k} + \Delta c\phi_{i-1,j}^{k+1}, \\
&j = N: && -2\Delta F\phi_{i,N-1}^{k+1} + (2\Delta F + \Delta c + 1)\phi_{i,N}^{k+1} = \phi_{i,N}^{k} + \Delta c\phi_{i-1,N}^{k+1};
\end{aligned} \tag{49}$$

$$\Delta c = u_j\frac{\Delta t}{\Delta x}, \quad \Delta F = \alpha\frac{\Delta t}{\Delta y^2}, \quad \Delta R = \frac{a}{R}\Delta F\,\Delta y.$$

By use of the usual Taylor series expansions, it was verified that the finite difference equations (49) are compatible with the governing partial differential equations with truncation error = $O(\Delta x) + O(\Delta y) + O(\Delta t)$.

A stability analysis demonstrated the unconditional stability of the equations (49). While solving (49), the

finite increments, Δx, Δy, and Δt, were reduced to the point where the solution became independent of increment size.

The structure of the equation (23) dictates a marching type of solution, in both x and t, for the equations (49). To begin the solution one starts at $t = 1\,\Delta t$ and at $x = 1\,\Delta x$ with the initial condition ($t = 0$) and the inlet boundary condition supplying the information needed to cause (49) to be a set of N simultaneous algebraic equations which are then solved for the nodal temperatures at $x = 1\,\Delta x$ and $t = 1\,\Delta t$. With these one can proceed to $x = 2\Delta x$ and solve the simultaneous equations again, still at $t = 1\,\Delta t$. This is continued until the x of interest is reached. The entire process is repeated at $t = 2\,\Delta t$, etc., until the time of interest or the steady-state, if there is one, is reached.

RESULTS AND DISCUSSION

The improved quasi-steady approach response functions for the step change in inlet temperature, (34), (35) and (38), and for the sinusoidal inlet fluid temperature variation, (40), (43) and (44), contain various integrals of the Airy function which were computed numerically with the Airy function values taken from [19]. With this, the values of the response functions of the improved quasi-steady model for the step change in inlet temperature were evaluated and are given as the solid curves in Figs. 1–4. Examination of (34) and (35) indicates dependence of the wall temperature excess ratio and the non-dimensional surface flux on a single variable, $\phi_0\tau/(3\chi)^{1/3}$, which combines the χ and τ dependence. To test the accuracy of the method, the finite difference solution to the same problem was run. The finite difference equations and solutions exhibit a dependence of the wall temperature and flux on $\phi_0\tau/(3\chi)^{1/3}$ and a separate dependence on χ and on $a = \rho c_p R/\rho_w c_{pw} b$ which is the ratio of the thermal capacity of the fluid to that of the wall, both on a per unit length in x basis. So, finite difference solutions were carried out for a range of values of a. Figure 1 shows the results for $a = 0.1$ with the various symbols representing the correct solution, the finite difference solution, at various values of χ chosen for convenience of the finite difference solution. As is evident from the figure, the improved quasi-steady result exhibits excellent agreement with the finite difference result for $a = 0.1$ over the range of χ which more than spans the thermal entrance region. Also presented in the same figure, as dashed lines, are the predicted responses using the standard quasi-steady approach, equations (45) and (46). As can be seen from these equations, there is a separate dependence upon the group $a\chi^{2/3}$. However, for $a = 0.1$, the curves for the smallest and largest value of χ used are nearly coincident so that only the one for the lowest value of χ was plotted and this curve is very close to the curve for $\chi = 0$ when $a = 0.1$. Examination of Fig. 1 indicates that the standard quasi-steady approach does not do too well, even at this relatively low value of a, in predicting the correct responses given by the finite difference solution.

Now, at $a = 0.1$ the thermal capacity of the wall material is dominant and that of the fluid is much less important. However, as a increases, the fluid's thermal capacity becomes a more and more significant factor controlling the response functions and since the improved quasi-steady approach takes finite fluid thermal capacity into approximate account for non-slug flows, one expects increasing deviation between the proposed method and the finite difference results for the larger values of a. This can be seen by reference to Fig. 2, $a = 0.5$, and Fig. 3 for which $a = 1.0$. In Fig. 2, the agreement between the proposed method (solid lines) and the finite difference result, while not as satisfying as that of Fig. 1, is still considered quite good. Showing up in this figure is the rise, in the finite difference predictions, of the heat flux from zero at values of $\phi_0\tau/(3\chi)^{1/3}$ near zero. The actual heat flux, especially at the larger values of χ, is lower and the wall temperature at the highest χ is larger than those calculated by the improved quasi-steady approach at small values of $\phi_0\tau/(3\chi)^{1/3}$. This is caused by the fact that, with the actual linear velocity profile, the wall is preheated by fluid layers moving faster than u_m since these layers arrive at any x before fluid moving at u_m

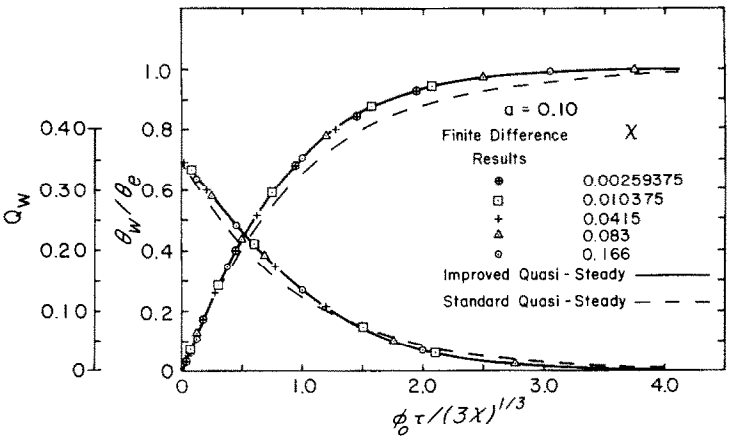

FIG. 1. Wall temperature and heat flux responses for a step change in inlet temperature.

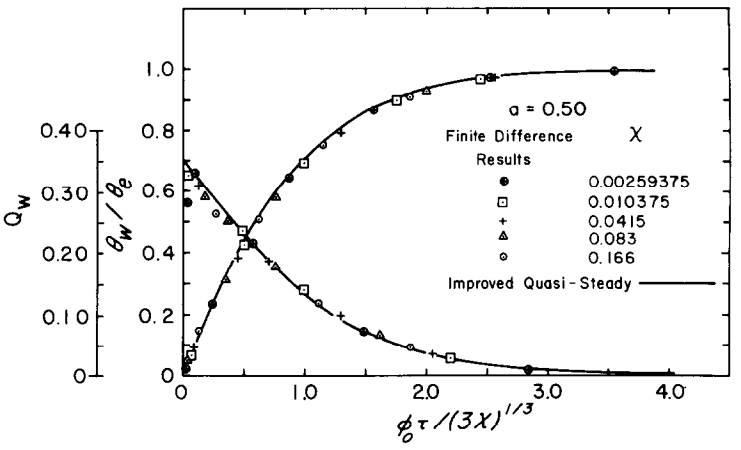

FIG. 2. Wall temperature and heat flux responses for a step change in inlet temperature.

and communicate thermally with the wall by y conduction. This raises the wall temperature slightly, in advance of $t = x/u_m$, for the largest values of χ, which, it is felt, is at least part of the reason for the lower actual flux. Essentially, this is part of the intermediate time domain, referred to earlier, in which fluid that satisfies the initial condition is communicating with fluid that satisfies the inlet condition. In Fig. 3, for which $a = 1.0$, the trends, first seen in Fig. 2, are even more apparent. The agreement displayed between the improved quasi-steady predictions and those of the finite difference method is considered satisfactory. Tentatively, it is suggested that $a = 1.0$ be considered as the upper limit of the improved quasi-steady approach in terms of acceptable engineering accuracy. Additional evidence for this domain of validity conclusion is available from finite difference results at $a = 0.75$, 1.5, and 4.5, not presented herein.

Also shown in Fig. 3 via dashed lines, for the two extreme values of χ, are the standard, simple, quasi-steady solutions, (45) and (46). The overall agreement between these solutions and the finite difference results is not very good especially at the higher value of χ. In Fig. 1, the error in the standard quasi-steady solution was due almost exclusively to thermal history effects, since the group containing $a\chi^{2/3}$ in equations (45) and (46) is virtually zero, while the additional shift upward of the dashed curve for $\chi = 0.166$ in Fig. 3 is due to the larger values of $a\chi^{2/3}$ which represents an incorrect dependence upon finite fluid thermal capacity.

Figure 4 compares the bulk mean temperature predictions of the present method, equation (38), for the step change in inlet temperature, to those of the finite difference method. The agreement is very good except at low values of $\phi_0\tau/(3\chi)^{1/3}$ for the higher χ where the finite difference results are higher for θ_B because of the lower surface flux as explained earlier.

On the basis of the first four figures, it is seen that the improved quasi-steady approach, which attempts to take into account both thermal history and fluid thermal capacity effects, predicts the finite difference results reasonably well and does significantly better than the standard quasi-steady approach. Yet the improved quasi-steady approach, though more difficult to apply than is the standard quasi-steady solution, is a considerably easier approach than is the

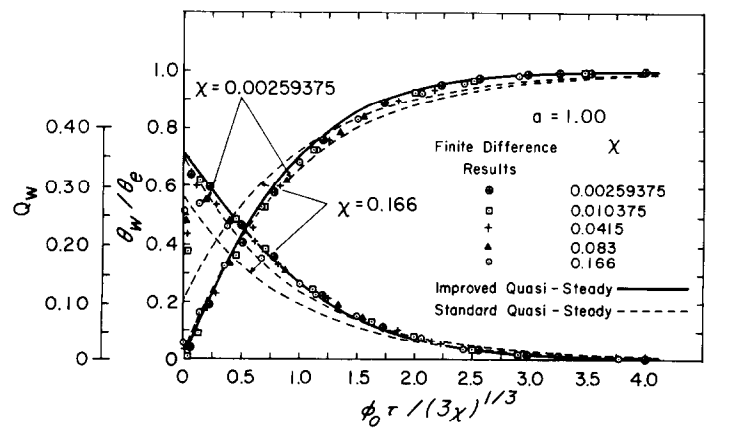

FIG. 3. Wall temperature and heat flux responses for a step change in inlet temperature.

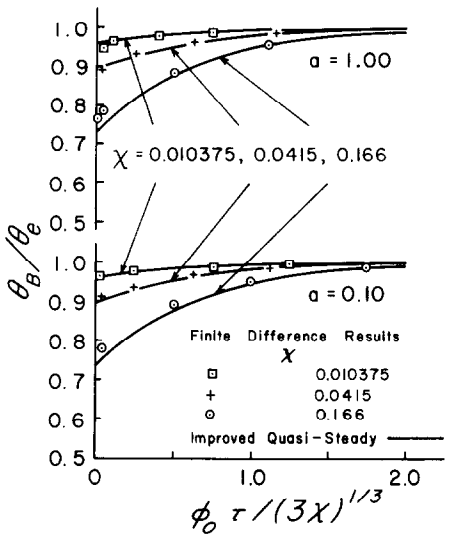

FIG. 4. Fluid bulk mean temperature response for a step change in inlet temperature.

finite difference solution to the problem. Once the finite difference equations were derived and programmed properly for the computer, some individual runs, for one value of a and two of the largest χ values, required 2000 s or 34 CRU for the step change in inlet temperature. By way of contrast, the computer program which evaluates the improved quasi-steady response functions (34), (35) and (38) required only a total time of 10 s or 1 CRU to complete all of the calculations.

Sinusoidal inlet temperature variation

For this inlet temperature some representative results for the wall temperature, surface heat flux, and bulk mean temperature are given in Figs. 5 and 6. The one value of $b^*\chi^{1/3}$ for which finite difference results are presented here was chosen to provide the most severe test for the improved quasi-steady approach.

Looking at Fig. 5, one sees that the improved quasi-steady results for the surface temperature and heat flux are in very good agreement with the finite difference results in both the transient start-up and the ultimate periodic state for the parameter values that were selected. The standard quasi-steady approach, however, differs significantly from the finite difference result. Since the periodic state has been reached within the first cycle, all cycles beyond the second are the same as the second. Figure 6 displays the results for the bulk mean temperature in the eventual periodic unsteady state.

CONCLUDING REMARKS

An improved quasi-steady approach, which takes into approximate account both thermal history and thermal capacity of the fluid, is developed for transient, conjugated forced convection problems. Using this approach, two analytical solutions are found, for a linear velocity profile, to transient conjugated problems in the thermal entrance region of a duct and the predicted wall temperature, surface heat flux, and local bulk mean temperature of the fluid are compared to finite difference solutions and to standard quasi-steady solutions to the same problems. Agreement of the proposed improved quasi-steady approach with the finite difference solution is highly satisfactory for a reasonably wide range of the parameter, a, which is the ratio of the thermal capacity of the fluid to that of the solid wall, while the standard quasi-steady approach leads to substantial error.

It is also seen that the method developed herein, which is an exact solution for transient slug flows and in the limit of the steady-state is also an exact solution for non-slug flows, is easier to deal with and more economical to use than is a finite difference solution to the problem. Often a needed kernel, which is related to

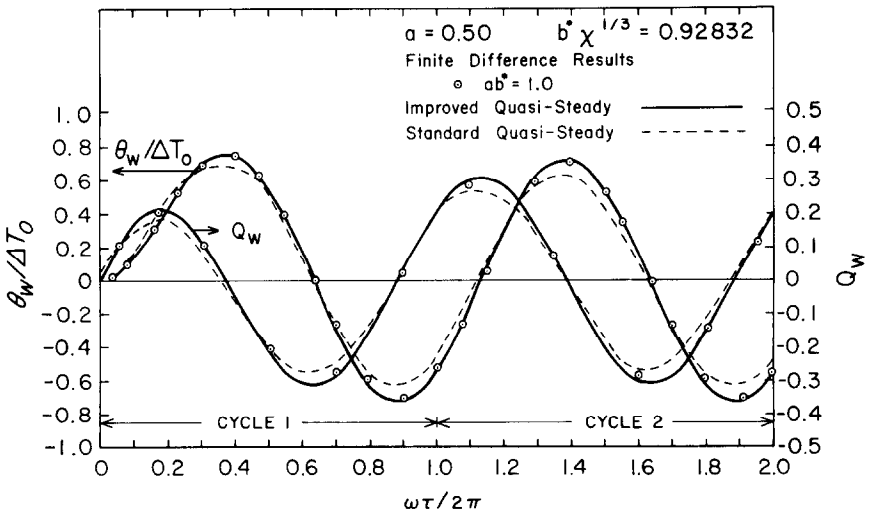

FIG. 5. Wall temperature and heat flux responses for an inlet temperature varying sinusoidally with time.

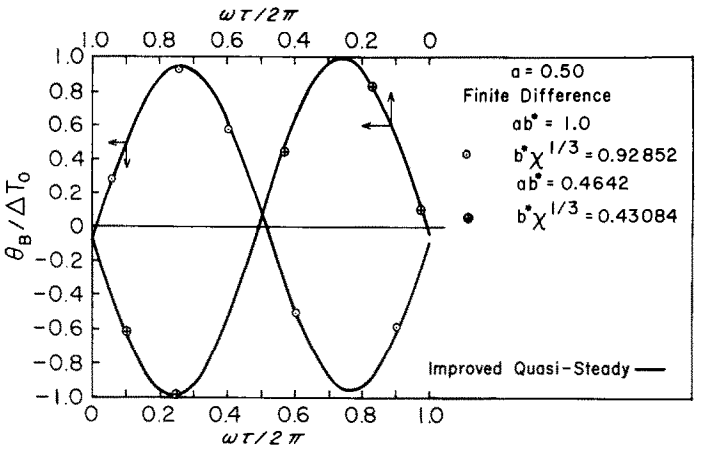

FIG. 6. Fluid bulk mean temperature response, in the periodic state, for an inlet temperature varying sinusoidally with time.

the steady-state flux for flow over the same surface when isothermal, is already available from solution or experiment.

Acknowledgement—This material is based upon work supported by the National Science Foundation under grant No. ENG-77-18268 and the author wishes to express his thanks for their support.

REFERENCES

1. D. E. Adams and B. Gebhart, Transient forced convection from a flat plate subjected to a step energy input, *J. Heat Transfer* **86,** 253–258 (1964).
2. R. Siegel and M. Perlmutter, Laminar heat transfer in a channel with unsteady flow and wall heating varying with position and time, *J. Heat Transfer* **85,** 358–365 (1963).
3. R. Siegel, Forced convection in a channel with wall heat capacity and with wall heating variable with axial position and time, *Int. J. Heat Mass Transfer* **6,** 607–620 (1963).
4. K. Namatame, Transient temperature response of an annular flow with step change in heat generating rod, *J. nucl. Sci. Tech.* **6,** 591–600 (1969).
5. J. Sucec, Unsteady heat transfer between a fluid, with time varying temperature, and a plate: An exact solution, *Int. J. Heat Mass Transfer* **18,** 25–36 (1975).
6. M. Soliman and H. A. Johnson, Transient heat transfer for turbulent flow over a flat plate of appreciable thermal capacity and containing time dependent heat source, *J. Heat Transfer* **89,** 362–370 (1967).
7. M. Soliman and H. A. Johnson, Transient heat transfer for forced convection flow over a flat plate of appreciable thermal capacity and containing an exponential time dependent heat source, *Int. J. Heat Mass Transfer* **11,** 27–38 (1968).
8. H. Kawamura, Analysis of transient turbulent heat transfer in an annulus, Part I: Heating element with a finite (non-zero) heat capacity and no thermal resistance, *Heat Transfer, Japan. Res.* **3,** 45–68 (1974).
9. H. Kawamura, Experimental and analytical study of transient heat transfer for turbulent flow in a circular tube, *Int. J. Heat Mass Transfer* **20,** 443–450 (1977).
10. A. Sh. Dorfman, Solution of the external problem of unsteady state convective heat transfer with coupled boundary conditions, *Int. chem. Engng* **17,** 505–510 (1977).
11. R. Karvinen, Steady state and unsteady heat transfer between a fluid and a flat plate with coupled convection, conduction and radiation, *Acta polytech. scand. (ser. e)* **73,** 5–36 (1976).
12. R. Karvinen, Some new results for conjugated heat transfer in a flat plate, *Int. J. Heat Mass Transfer* **21,** 1261–1264 (1978).
13. T. E. W. Schumann, Heat transfer: A liquid flowing through a porous prism, *J. Franklin Inst.* **208,** 405–416 (1929).
14. G. E. Roberts and H. Kaufmann, *Tables of Laplace Transforms*, W. B. Saunders, Philadelphia, PA (1966).
15. W. M. Kays, *Convective Heat and Mass Transfer*, McGraw-Hill, New York (1966).
16. R. Siegel, Heat transfer for laminar flow in ducts with arbitrary time variations in wall temperature, *J. appl. Mech.* **27,** 241–249 (1960).
17. M. J. Lighthill, Contributions to the theory of heat transfer through a laminar boundary layer, *Proc. R. Soc., Lond. (Ser. A)* **202,** 359–377 (1950).
18. Y. L. Luke, *Integrals of Bessel Functions*, McGraw-Hill, New York (1962).
19. M. Abramowitz and I. A. Stegun (Editors), *Handbook of Mathematical Functions with Formulas, Graphs, and Mathematical Tables*, National Bureau of Standards Applied Math. Series 55 (1964).
20. M. N. Özisik, *Boundary Value Problems of Heat Conduction*, International Textbook, Scranton, Penn. (1968).
21. E. M. Sparrow and F. N. DeFarias, Unsteady heat transfer in ducts with time varying inlet temperature and participating walls, *Int. J. Heat Mass Transfer* **11,** 837–853 (1968).
22. J. Sucec, Transient heat transfer between a plate and a fluid whose temperature varies periodically with time, *J. Heat Transfer* **102,** 126–131 (1980).

APPENDIX A

Inversion of equation (31)

Needed is $$\underset{s\to\chi}{L^{-1}}\left(\frac{1}{s}e^{-\phi_0 s^{1/3}\tau}\right). \tag{A.1}$$

Viewing the bracketed term in (A.1) as being a function of $s^{1/3}$, we attempt to make use of the following result from [14].

$$\underset{s\to\chi}{L^{-1}}\, g[w(s)] = \int_0^\infty r(u,\chi) f(u)\, du, \tag{A.2}$$

where

$$f(u) = \underset{w\to u}{L^{-1}}\, g[w] \quad \text{and} \quad r(u,\chi) = \underset{s\to\chi}{L^{-1}}\, e^{-uw(s)}.$$

Identifying $w(s)$ as $s^{1/3}$ in (A.1) gives

$$g[w] = \frac{1}{w^3} e^{-\phi_0 \tau w}. \quad \text{(A.3)}$$

Using the translation theorem and a transform table [14] on (A.3) yields

$$f(u) = 0 \text{ for } u < \phi_0\tau, \text{ and } \frac{(u-\phi_0\tau)^2}{2} \text{ for } u > \phi_0\tau. \quad \text{(A.4)}$$

Rearranging, using a substitution property and tables of inverses in [14] gives,

$$L_{s\to\chi}^{-1} e^{-us^{1/3}} = L_{s\to\chi}^{-1} e^{-3(u^3 s/27)^{1/3}} = 27\frac{F\left(\frac{27\chi}{u^3}\right)}{u^3},$$

where $F(\chi) = L_{s\to\chi}^{-1} e^{-3s^{1/3}} = \frac{\sqrt{3}}{\pi\chi^{3/2}} K_{1/3}\left(\frac{2}{\sqrt{\chi}}\right)$,

where K is a modified Bessel function of the second kind. With this, one has

$$r(u,\chi) = \frac{u^{3/2}}{3\pi\chi^{3/2}} K_{1/3}\left(\frac{2}{3}\frac{u^{3/2}}{\sqrt{3\chi}}\right). \quad \text{(A.5)}$$

Using (A.5) and (A.4) in (A.2) yields the inverse needed in (A.1) as the second term in equation (32).

UNE APPROCHE QUASI-PERMANENTE AMELIOREE DES PROBLEMES VARIABLES DE CONVECTION FORCEE AVEC COUPLAGE

Résumé—On présente une méthode, dite approche quasi-permanente améliorée, qui tient compte à la fois de l'effet de l'histoire thermique et du stockage de l'énergie thermique d'un fluide en écoulement pour des problèmes de convection avec couplage, et qui s'applique avec deux des hypothèses, ordinairement implicite, dans l'approche usuelle, simple, quasi-permanente, des problèmes de ce genre. Le développement de la méthode est facilité par une transformation de variable qui conduit à une solution exacte pour les écoulements-pistons et qui est généralisée (et approximativement valable) pour les écoulements à profil varié.

On présente deux solutions analytiques obtenues par cette méthode et on les compare aux solutions par différences finies. Des comparaisons additionnelles sont faites avec les résultats classiques quasi-permanents.

EINE ERWEITERTE METHODE ZUR QUASI-STATIONÄREN BEHANDLUNG VON INSTATIONÄREN KONJUGIERTEN PROBLEMEN DER ERZWUNGENEN KONVEKTION

Zusammenfassung—Es wird eine Methode der erweiterten quasi-stationären Behandlung besechrieben, die bei instationären konjugierten Problemen der erzwungenen konvektion sowohl den Einfluß der thermischen Vorgeschichte wie auch die thermische Energiespeicherfähigkeit eines strömenden Fluids näherungsweise berücksichtigt und damit auf zwei der Annahmen verzichtet, die gewöhnlich bei der üblichen einfachen quasi-stationären Behandlung solcher Probleme gemacht werden. Zur Erweiterung der Methode wird eine Variablentransformation vorgeschlagen, die zu einer exakten Lösung für Pfropfenströmungen führt. Diese wird dann verallgemeinert und damit auch näherungsweise für Nicht-Pfropfenströmungen gültig. Zwei analytische Lösungen, bei denen die vorgeschlagene Methode benutzt wurde, werden angegeben und mit numerischen Lösungen verglichen, die als Vergleichsgrundlage erstellt wurden. Zusätzliche Vergleiche wurden mit Ergebnissen der üblichen einfachen quasi-stationären Methode durchgeführt.

УСОВЕРШЕНСТВОВАННЫЙ КВАЗИСТАЦИОНАРНЫЙ МЕТОД АНАЛИЗА НЕСТАЦИОНАРНЫХ СОПРЯЖЕННЫХ ЗАДАЧ ВЫНУЖДЕННОЙ КОНВЕКЦИИ

Аннотация — Предложен усовершенствованный квазистационарный метод, учитывающий как влияние предистории потока жидкости, так и его тепловой энергии в нестационарных сопряженных задачах вынужденной конвекции, что позволяет не прибегать к использованию двух допущений, характерных для обычного простого квазистационарного метода решения таких задач. Усовершенствованный метод основан на преобразовании переменной и позволяет получить точное решение для стержневых режимов течения, которое можно обобщить с достаточной степенью точности и на другие режимы течения.

Предложенным методом получено два аналитических решения и дано сравнение со специально выполненными решениями методом конечных разностей. Кроме того, проведено сопоставление с обычными стандартными квазистационарными результатами.